Molar Heat Capacity at Constant Volume for Isobutane at Temperatures from (114 to 345) K and at Pressures to 35 MPa[†,‡]

Richard A. Perkins and Joseph W. Magee*

Thermophysical Properties Division, Chemical Science and Technology Laboratory, National Institute of Standards and Technology, Boulder, Colorado 80305-3337

Molar heat capacities at constant volume (C_V) were measured with an adiabatic calorimeter for pure isobutane. The high purity of the samples was verified by chemical analysis. Temperatures ranged from the triple point of isobutane near 114 K to the upper temperature limit of the calorimeter at 345 K, whereas pressures ranged up to 35 MPa. Measurements were conducted on liquid in equilibrium with its vapor and on compressed liquid samples along isochores. Heat capacity results are reported for two-phase ($C_V^{(2)}$), saturated liquid (C_σ), and single-phase (C_V) isochores. Vapor pressure data are reported that are based on measurements of $C_V^{(2)}$ along a two-phase isochore. Measurements were also made to determine the triple-point temperature of (113.707 ± 0.030) K and enthalpy of fusion of (4494 ± 20) J·mol^{-1} for isobutane near its triple point. The principal sources of uncertainty are the temperature rise measurement and the change-of-volume work adjustment. The expanded uncertainty (i.e., a coverage factor $k = 2$ and thus a two-standard deviation estimate) for values of $C_V^{(2)}$ is estimated to be 0.5 %, for C_σ it is 0.7 %, and for C_V it is 0.7 %.

Introduction

Isobutane is a common hydrocarbon fuel and is a key component of liquefied petroleum gas (LPG) and natural gas mixtures; it is also widely used as a component in mixtures for refrigeration cycles. The isochoric heat capacity of a fluid may be calculated from knowledge of its ideal gas properties and an equation of state that represents the relationship between temperature (T), pressure (P), and density (ρ). The isochoric heat capacity is given by

$$C_V - C_V^0 = -T\int_0^\rho \left(\frac{\partial^2 P}{\partial T^2}\right)_\rho \frac{\mathrm{d}\rho}{\rho^2} \quad (1)$$

where C_V^0 is the ideal gas heat capacity. The isochoric derivative $(\partial^2 P/\partial T^2)_\rho$ is known to possess small absolute values, except in the vicinity of the critical point, and is difficult to measure directly. Equation 1 provides a means to check for consistency between independent measurements of density and heat capacity, usually through an equation of state.

Molar heat capacity was measured with an adiabatic calorimeter at saturated liquid and single-phase compressed liquid state conditions. These measurements cover temperatures from the triple point to 345 K, with compressed liquid isochores at pressures up to 35 MPa. The triple-point temperature, enthalpy of fusion, and vapor pressures are reported on the basis of the evaluation of two-phase heat capacity measurements at temperatures from below the triple point to 345 K.

Experimental Section

Materials. The isobutane sample used in this work was specified by the supplier as having a purity of 99.99 % (molar basis), as determined by gas chromatography−mass spectrometry analysis. As shown by its certificate of chemical analysis, the principal impurities are isobutylene (25.1 ppm), 1-butene (15.4 ppm), and *n*-butane (15.2 ppm). Measurements of the triple-point temperature described here on this isobutane sample are consistent with this purity.

Measurements. The adiabatic calorimeter that was used for these measurements was originally described by Goodwin[1] to study hydrogen heat capacity and was used to measure the heat capacity of light hydrocarbons including methane,[2] ethane,[3] (methane + ethane) mixtures,[4] and propane.[5] The calorimeter was improved by Magee[6] prior to measurements on butane.[7] Recent measurements on a very high purity sample of propane[8] allowed the volume of the calorimeter to be recalibrated with an uncertainty of 0.012 %, which reduces the uncertainty in the present results for both heat capacity and density. The two-phase heat capacity data are used to generate vapor pressure data down to the triple-point temperature, and the triple-point temperature and the associated enthalpy of fusion are reported here.

Details of the calorimeter cell are described in detail by Goodwin[1] and Magee.[6] The present automated data acquisition and control systems are discussed in detail by Magee.[6] The calorimeter consists of a nearly adiabatic cell (also called a calorimetric bomb) that is spherical and has been operated at temperatures from (14 to 345) K at pressures up to 35 MPa. During a measurement, a sample of well-established mass is confined within the cell with a well-known volume (approximately 77 cm^3); as shown by Magee[6] and Perkins et al.,[8] the exact volume varies with both temperature and pressure. After a precisely measured quantity of electrical energy (Q) pulse is applied and the cell temperature equilibrates, the resulting temperature increase ($\Delta T = T_1 - T_2$) is measured. We found the molar heat capacity at constant volume (C_V) of the sample by subtracting the energy required to heat the empty cell (Q_0) and the pressure−volume work (W_{PV}) as

[†] Part of the "William A. Wakeham Festschrift".

* Corresponding author. E-mail: joe.magee@nist.gov.

10.1021/je9001575
Published on Web 06/04/2009

$$C_V = \left(\frac{\partial U}{\partial T}\right)_V \cong \frac{Q - Q_0 - W_{PV}}{n\Delta T} \quad (2)$$

To fill the cell, sample gas was condensed into the cold sample cell until both the cell temperature and pressure reached plateau values when the cell was completely filled. Then, the charge valve was closed, and the cell and its contents were cooled to the starting temperature. A small quantity of gas was slowly vented to an exhaust stack until the pressure fell to the starting value. A series of heating cycles was started and continued until the upper temperature limit of 345 K was reached or until the maximum pressure of 35 MPa was reached for single-phase samples. At the completion of an isochore, some of the sample was discharged into a collection cylinder to obtain the next filling density. The increment of mass discharged was determined from difference weighings of the collection cylinder after a buoyancy correction was applied. Following the last isochore, the sample remaining in the cell was collected and weighed. For each isochoric run, the mass of sample was determined from the sum of all mass increments that were measured after that run. A series of such isochores at different densities (ρ) completed the $C_V(\rho,T)$ surface for the sample.

The energy required to heat the empty cell (Q_0) from the initial temperature (T_1) to the final temperature (T_2) was found from previous experiments with the cell thoroughly evacuated.[6] The fit for these empty cell results is described by Magee[6] and is the basis for evaluation of Q_0 in the analysis of the present measurements with eq 2. The pressure−volume work (W_{PV}) accounts for the work done by the fluid on the thin-walled cell as the pressure rises from P_1 to P_2. Calculation of the pressure−volume work is discussed by Goodwin and Weber[9] and is given by

$$W_{PV} = \left(T_2\left(\frac{\partial P}{\partial T}\right)_{V_2} - \frac{\Delta P}{2}\right)\Delta V \quad (3)$$

where $\Delta P = P_2 - P_1$ is the pressure rise and $\Delta V = V_2 - V_1$ is the volume increase. The pressure derivative in eq 3 has been calculated with the equation of state of Bücker and Wagner.[10]

The amount (mol) of substance, n, contained in the cell varies slightly because of the noxious volume, which is about 0.2 % of the cell volume.[6] This noxious volume is the sum of the volumes of the pressure transducer, charging valve, and interconnecting capillary tubing. The pressure transducer and valve are contained in an isothermal aluminum block that is controlled at a temperature near 320 K such that the temperature gradient occurs along a thin capillary (ID = 0.13 mm) tube between the cell and the pressure transducer + valve assembly. The amount (mol) of the sample in this noxious volume is obtained from the measured volumes and the density calculated with the equation of state[10] at the measured pressure and temperature of the pressure transducer plus valve assembly and by assuming a quadratic temperature profile along the length of the capillary. The molar mass for isobutane of 58.122 $g \cdot mol^{-1}$, based on the atomic weights of the elements,[11] was used throughout this work.

Results

Triple-Point Temperature. Measurements of the triple point of isobutane provide a check of the purity of the sample because an impure sample will exhibit freezing point depression. The triple-point temperature of isobutane has been studied by Aston et al.,[12] who reported a value of (113.747 ± 0.05) K converted from the IPTS-27 temperature scale to the ITS-90 scale. Aston et al.[12] observed a depression in the freezing point that indicated molar impurities on the order of 0.0015 mol percent in their isobutane sample. Parks et al.[13] reported (113.207 ± 0.7) K, Das et al.[14] reported 113.56 K, Rossini et al.[15] reported 113.57 K, and Francis[16] reported 113.75 K, where all values have been converted to the ITS-90 scale. The value of (113.730 ± 0.010) K was recently measured by Glos et al.[17] for the triple-point temperature of a 99.97 % pure sample of isobutane. It is the value of Glos et al.[17] that has been adopted for the equation of state of Bücker and Wagner[10] for isobutane.

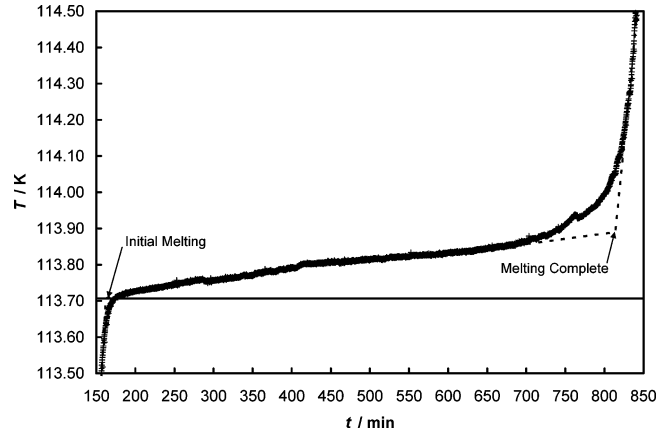

Figure 1. Measured calorimeter temperatures as isobutane was slowly melted near its triple point: +, measured temperature; line at $T = 113.707$ K, measured triple-point temperature of this sample.

The present isobutane sample is 99.99 % pure relative to the 99.9985 % pure sample studied by Aston et al.,[12] so there is more freezing point depression in the measurements reported here. Figure 1 shows the measured temperature as a function of time that we observed for isobutane near its triple point. The temperature increases with elapsed heating time as more of the sample melts. This temperature increase is due only in part to freezing point depression; most of the temperature increase is due to temperature gradients across the liquid layer between the heated calorimeter vessel and the remaining solid sample. The experiment shown in Figure 1 was optimized for accurate determination of the enthalpy of fusion reported below. However, the temperature rise can be extrapolated to the start of melting to provide an estimate of the triple-point temperature of isobutane that corresponds to a very small melt fraction, where freezing point depression is expected to be the largest. We measured a temperature of (113.707 ± 0.005) K for the initial melting temperature of this 99.99 % pure sample of isobutane that does not account for freezing point depression. Temperature measurement noise is about 0.003 K. Our initial melting temperature is lower than the measurements of Aston et al.[12] and Glos et al.,[17] who report values of (113.747 ± 0.05) K and (113.730 ± 0.010) K, respectively. It is likely that a difference of (0.02 to 0.04) K between the present initial melting temperature and these published values for the triple-point temperature is primarily due to freezing point depression. Raw data from our scanning experiments simply does not lend itself to characterizing the melt temperature as a function of fraction melted, such as Aston et al.[12] were able to do for a purer sample of isobutane. Because our result is an extrapolation, its uncertainty is estimated to be ± 0.030 K. Therefore, we report a value of (113.707 ± 0.030) K for our determination

Table 1. Isochoric Heat Capacities, C_V, of Isobutane at Temperatures from (120 to 345) K at Pressures to 35 MPa

T / K	ρ / mol·L^{-1}	P / MPa	C_V / J·mol^{-1}·K^{-1}	T / K	ρ / mol·L^{-1}	P / MPa	C_V / J·mol^{-1}·K^{-1}
119.824	12.679	6.500	71.22	294.138	10.171	24.048	99.10
124.969	12.662	15.325	72.14	298.278	10.165	26.943	99.99
130.018	12.643	25.536	73.32	302.393	10.159	29.793	100.74
122.330	12.671	10.732	71.61	306.498	10.153	32.612	102.04
127.431	12.652	20.667	72.63	266.606	10.211	4.054	92.14
132.429	12.636	28.973	73.82	270.879	10.205	7.235	92.99
141.365	12.331	4.922	73.32	275.117	10.199	10.363	94.06
146.265	12.315	13.401	74.25	279.338	10.192	13.450	95.20
151.090	12.299	21.305	75.18	283.538	10.186	16.491	96.18
155.838	12.285	28.673	76.28	287.716	10.180	19.487	97.22
143.716	12.323	9.088	73.74	291.871	10.174	22.438	98.44
148.585	12.307	17.196	74.72	296.012	10.168	25.350	99.94
153.376	12.293	24.872	75.69	300.136	10.162	28.222	100.48
162.300	11.989	4.549	75.71	304.247	10.156	31.058	101.52
167.029	11.976	11.587	76.59	283.657	9.842	2.372	95.67
171.692	11.963	18.296	77.43	287.933	9.836	5.135	96.68
176.294	11.951	24.825	78.43	292.183	9.831	7.863	98.07
180.830	11.939	31.062	79.80	296.421	9.825	10.563	98.75
164.597	11.983	8.126	76.26	300.638	9.820	13.229	100.03
169.293	11.970	14.798	77.08	304.846	9.814	15.868	101.01
173.926	11.957	21.461	78.06	309.040	9.809	18.478	102.38
178.500	11.945	27.869	78.99	313.228	9.803	21.063	102.98
183.242	11.645	4.049	78.07	317.393	9.798	23.611	103.51
187.834	11.633	9.994	79.02	321.547	9.793	26.133	104.78
192.378	11.622	15.769	79.81	325.699	9.787	28.633	106.08
196.863	11.611	21.369	81.16	329.842	9.782	31.107	106.78
201.308	11.601	26.822	81.98	333.968	9.777	33.555	107.88
205.687	11.591	32.085	83.13	285.763	9.839	3.730	96.28
185.448	11.639	6.869	78.63	290.038	9.834	6.483	97.37
190.011	11.628	12.743	79.62	294.296	9.828	9.205	98.00
194.515	11.617	18.415	80.61	298.534	9.822	11.894	98.97
198.974	11.607	23.939	81.69	302.754	9.817	14.551	100.42
203.378	11.596	29.282	82.49	306.975	9.811	17.187	101.25
203.616	11.304	3.700	80.96	311.165	9.806	19.783	102.14
208.089	11.294	8.785	82.04	315.352	9.801	22.355	103.37
212.530	11.285	13.758	83.00	319.529	9.795	24.899	104.29
216.918	11.276	18.597	83.89	323.688	9.790	27.412	105.09
221.262	11.266	23.313	85.00	327.840	9.785	29.902	106.30
225.572	11.258	27.916	85.85	331.979	9.779	32.367	107.91
229.830	11.249	32.388	86.73	303.811	9.423	2.271	99.83
205.821	11.299	6.192	81.19	308.123	9.418	4.631	100.80
210.261	11.290	11.205	82.36	312.423	9.413	6.973	101.82
214.660	11.280	16.095	83.42	316.705	9.408	9.293	102.97
219.020	11.271	20.866	84.44	320.980	9.403	11.596	104.60
223.328	11.262	25.507	85.63	325.247	9.398	13.880	105.73
227.602	11.253	30.036	86.44	329.508	9.393	16.147	106.45
224.207	10.949	3.209	84.09	333.759	9.388	18.392	107.16
228.594	10.940	7.563	85.18	337.998	9.383	20.617	108.51
232.950	10.932	11.833	86.15	342.233	9.378	22.826	110.23
237.259	10.924	16.001	87.31	306.067	9.420	3.504	100.71
241.536	10.916	20.084	88.35	310.381	9.415	5.860	101.98
245.774	10.908	24.074	89.40	314.682	9.410	8.197	102.64
249.980	10.900	27.977	90.18	318.978	9.405	10.517	103.88
254.151	10.893	31.797	91.18	323.266	9.400	12.819	104.79
226.505	10.944	5.490	84.53	327.539	9.395	15.099	105.76
230.859	10.936	9.783	85.57	331.807	9.390	17.362	106.57
235.183	10.928	13.991	86.65	336.062	9.385	19.603	107.61
239.464	10.920	18.103	87.79	340.310	9.381	21.824	108.42
243.715	10.912	22.131	88.62	344.554	9.376	24.029	109.59
247.921	10.904	26.062	89.81	312.622	9.223	2.143	102.01
252.106	10.897	29.918	91.01	316.946	9.218	4.329	103.28
244.913	10.582	2.940	87.70	321.275	9.213	6.508	104.19
249.240	10.575	6.667	88.84	325.586	9.209	8.668	104.99
253.542	10.567	10.334	89.74	329.891	9.204	10.815	106.10
257.801	10.560	13.926	90.58	334.190	9.199	12.947	107.66
262.027	10.553	17.452	91.98	338.485	9.195	15.066	108.51
266.232	10.546	20.919	93.11	342.772	9.190	17.169	109.53
270.404	10.539	24.318	94.15	314.809	9.220	3.247	102.19
274.555	10.533	27.659	95.07	319.151	9.216	5.436	103.12
278.680	10.526	30.942	95.99	323.482	9.211	7.612	104.96
246.876	10.579	4.626	88.13	327.822	9.206	9.782	105.71
251.174	10.571	8.311	89.23	332.136	9.201	11.928	106.39
255.440	10.564	11.931	90.33	336.448	9.197	14.061	107.61
259.679	10.557	15.488	91.30	340.748	9.192	16.177	108.82

Table 1. Continued

T / K	ρ / mol·L^{-1}	P / MPa	C_V / J·mol^{-1}·K^{-1}	T / K	ρ / mol·L^{-1}	P / MPa	C_V / J·mol^{-1}·K^{-1}
263.881	10.550	18.974	92.40	322.431	8.989	2.027	103.88
268.064	10.543	22.404	93.80	326.805	8.984	4.037	105.22
272.220	10.537	25.772	94.90	331.168	8.980	6.040	106.74
276.358	10.530	29.087	95.35	335.531	8.975	8.034	107.69
280.463	10.523	32.342	96.46	339.887	8.971	10.016	108.49
264.623	10.214	2.580	91.58	344.235	8.966	11.989	109.21
268.908	10.208	5.781	92.42	324.786	8.986	3.113	105.07
273.170	10.201	8.940	93.07	329.145	8.982	5.110	105.78
277.400	10.195	12.047	94.20	333.489	8.977	7.102	106.91
281.615	10.189	15.113	95.82	337.839	8.973	9.085	108.12
285.810	10.183	18.136	97.40	342.194	8.968	11.067	108.69
289.990	10.177	21.118	98.16				

of the triple-point temperature of isobutane, which is 0.04 K lower than Aston et al.[12] primarily because of freezing point depression.

Enthalpy of Fusion. The frozen sample was heated at a constant power of 0.0810 W while the temperature was recorded, as shown in Figure 1. We measured the enthalpy of fusion, $\Delta_{fus}H$, by integrating the applied heater power over the period of melting and applying corrections for heating of the calorimeter and parasitic heat losses. The onset of melting is indicated by a sudden decrease in the rate of temperature increase at fixed heating power. The measured temperature starts out near the triple-point temperature when melting begins but slowly increases as the thickness of the liquid layer increases between the cell wall and the melting solid. The temperature again rises more rapidly when the last solid has melted. The results and expanded uncertainties ($k = 2$) for $\Delta_{fus}H$ obtained from this experiment were (4494 ± 20) J·mol^{-1} at the triple point. These values agree well with those reported by Parks et al.[13] of (4498.6 ± 3) J·mol^{-1} but deviate by 47 J·mol^{-1} (1 %) from the values of Aston et al.[12] of (4541.3 ± 2) J·mol^{-1}, whose claimed error of ± 2 J·mol^{-1} represents their observed repeatability between multiple determinations rather than the uncertainty.

Isochoric Heat Capacity. The values measured for the isochoric heat capacity, C_V, of isobutane are given in Table 1 at 171 single-phase states. The average of the initial and final temperatures for each heating interval is given for the temperature (ITS-90) of each data point. The tabulated pressures are calculated from a least-squares fit of the (P,T) data by use of a seven-term function given by

$$P = \frac{c_1}{T_r^4} + \frac{c_2}{T_r^3} + \frac{c_3}{T_r^2} + \frac{c_4}{T_r} + c_5 + c_6\sqrt{T_r} + c_7 T_r \quad (4)$$

where the c_i are the fit coefficients for the isochore and $T_r = T/T_c$, where $T_c = 407.81$ K is the critical temperature of isobutane.[10] The density is calculated from the corrected

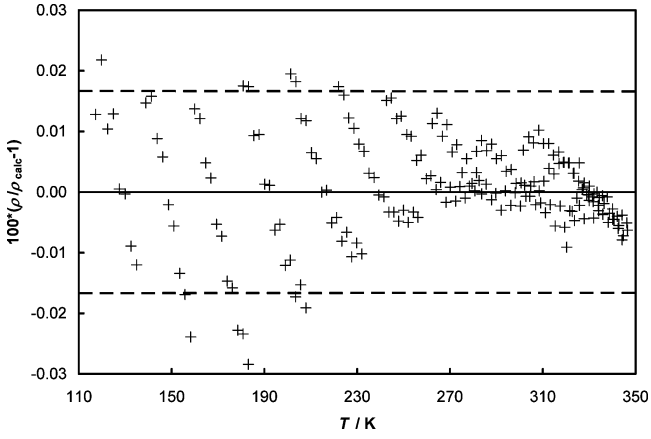

Figure 2. Relative deviations $100(\rho - \rho_{calcd})/\rho_{calcd}$ between the experimental densities in Table 1 and the densities calculated with the equation of state of Bücker and Wagner[10] at temperatures from (120 to 345) K and at pressures up to 35 MPa. The densities were calculated from the mass of sample and the calorimeter volume, which had been calibrated during separate measurements on propane.[8] The present data agree with the equation of state with a relative expanded uncertainty $u = 0.017$ % ($k = 2$), shown as dashed lines.

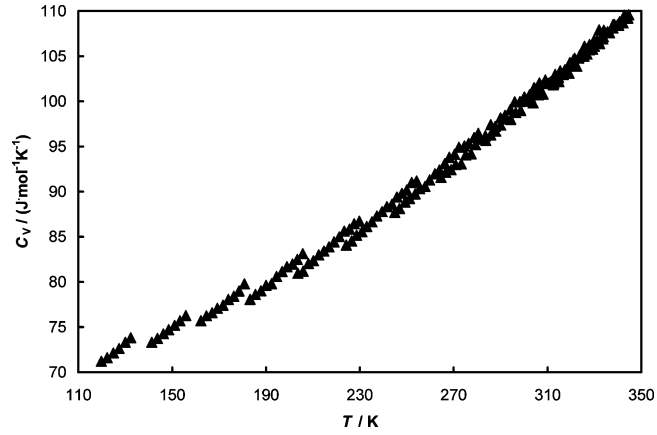

Figure 3. Measured isochoric heat capacities (C_V) of isobutane at temperatures from (120 to 345) K and at pressures up to 35 MPa.

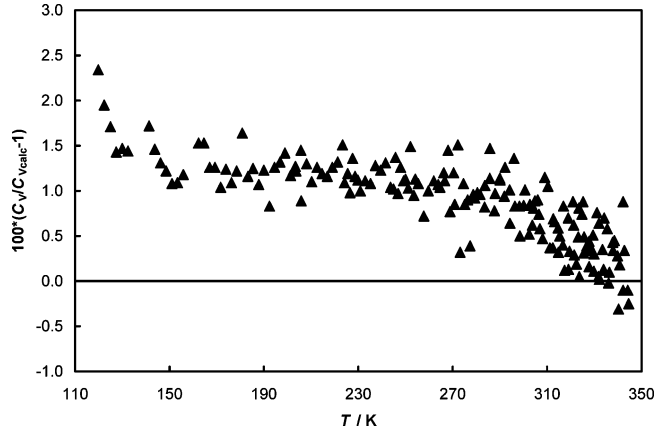

Figure 4. Relative deviations between measured isochoric heat capacities (C_V) of isobutane and values calculated with the equation of state of Bücker and Wagner[10] at temperatures from (120 to 345) K and at pressures up to 35 MPa: ▲, present results.

Table 2. Saturated Liquid Heat Capacities, C_σ, of Isobutane (0.70101 mol sample) at Temperatures from (117 to 316) K[a]

T / K	$\rho_{calcd,\sigma}$ / mol·L^{-1}	$P_{calcd,\sigma}$ / Pa	$C_V^{(2)}$ / J·mol^{-1}·K^{-1}	C_σ / J·mol^{-1}·K^{-1}	T / K	$\rho_{calcd,\sigma}$ / mol·L^{-1}	$P_{calcd,\sigma}$ / Pa	$C_V^{(2)}$ / J·mol^{-1}·K^{-1}	C_σ / J·mol^{-1}·K^{-1}
116.795	12.688	0.049607	99.974	99.973	119.574	12.643	0.096332	100.39	100.39
122.226	12.600	0.17596	100.86	100.86	124.959	12.555	0.317878	101.19	101.19
127.546	12.513	0.542256	101.83	101.83	130.235	12.470	0.921516	102.10	102.10
132.769	12.428	1.48619	102.54	102.54	135.417	12.385	2.39759	103.17	103.17
137.901	12.345	3.68596	103.69	103.68	140.511	12.302	5.68689	103.94	103.94
142.953	12.263	8.39707	104.41	104.41	145.522	12.221	12.4545	104.92	104.91
147.922	12.181	17.7517	105.31	105.30	150.467	12.140	25.4937	105.75	105.75
152.826	12.101	35.2272	106.17	106.16	155.336	12.060	49.0947	106.51	106.50
157.664	12.022	66.0854	107.02	107.02	160.145	11.981	89.7403	107.18	107.18
162.439	11.944	117.967	107.79	107.78	164.887	11.903	156.448	108.28	108.27
167.155	11.866	201.522	108.62	108.62	169.580	11.826	261.926	109.09	109.08
171.820	11.789	331.201	109.18	109.17	174.213	11.749	422.336	110.10	110.08
176.428	11.712	525.355	110.09	110.08	178.798	11.673	659.024	110.99	110.97
180.987	11.636	807.611	111.27	111.25	183.328	11.597	997.596	112.15	112.12
185.503	11.561	1207.3	112.03	112.00	187.820	11.522	1471.13	112.82	112.78
189.970	11.486	1758.51	112.85	112.81	192.258	11.447	2115.5	113.26	113.22
194.391	11.411	2501.96	113.77	113.72	196.656	11.373	2976.15	114.26	114.21
198.771	11.337	3485.33	114.82	114.75	201.014	11.299	4103.54	115.12	115.05
203.107	11.263	4760.96	115.69	115.61	205.337	11.225	5556.2	115.98	115.90
207.405	11.189	6389.87	116.45	116.35	209.614	11.151	7392.85	116.89	116.79
211.667	11.116	8438.9	117.50	117.40	213.859	11.078	9688.07	117.64	117.52
215.898	11.042	10 983.4	118.25	118.12	218.066	11.005	12 513.7	118.64	118.51
220.086	10.969	14 093	118.94	118.79	222.244	10.932	15 956.8	119.78	119.63
224.246	10.896	17 861.2	120.01	119.86	226.389	10.859	20 100.7	120.78	120.61
228.375	10.823	22 374.8	121.25	121.07	230.505	10.785	25 040.8	121.80	121.62
232.477	10.750	27 732.3	122.12	121.93	234.587	10.712	30 865.5	122.50	122.30
236.553	10.677	34 034.9	122.82	122.62	238.645	10.639	37 688.5	123.96	123.75
240.594	10.604	41 368.3	123.92	123.70	242.678	10.566	45 614.1	124.53	124.31
244.612	10.531	49 857.7	124.95	124.72	246.680	10.493	54 735.8	125.38	125.15
248.600	10.457	59 595.8	126.11	125.88	250.661	10.419	65 185.4	126.61	126.37
252.572	10.383	70 729.5	127.01	126.78	254.617	10.345	77 065.9	128.02	127.78
256.519	10.309	83 350.7	128.04	127.81	258.554	10.271	90 511.5	129.15	128.92
260.446	10.235	97 591.5	128.91	128.69	262.471	10.196	105 639	129.84	129.62
264.352	10.160	113 568	130.07	129.86	266.369	10.121	122 574	130.67	130.48
268.239	10.085	131 408	131.66	131.47	270.244	10.046	141 418	131.87	131.70
272.113	10.009	151 268	132.60	132.45	274.098	9.970	162 298	133.58	133.44
275.959	9.933	173 190	133.68	133.56	277.943	9.894	185 409	134.34	134.24
279.802	9.856	197 445	134.77	134.70	281.765	9.817	210 792	135.41	135.37
283.622	9.779	224 040	135.70	135.69	285.575	9.739	238 646	136.12	136.15
287.429	9.701	253 168	137.63	137.70	289.369	9.660	269 071	137.38	137.50
291.232	9.621	285 042	138.68	138.84	293.154	9.581	302 257	138.93	139.14
295.011	9.541	319 623	139.10	139.36	296.926	9.500	338 306	139.80	140.12
298.780	9.460	357 164	140.46	140.84	300.683	9.419	377 328	140.69	141.15
302.543	9.378	397 849	142.07	142.60	308.174	9.253	465 072	143.08	143.87
306.297	9.295	441 792	143.08	143.77	311.910	9.168	514 113	145.02	146.00
310.036	9.211	489 057	143.99	144.87	315.634	9.081	566 717	146.20	147.42
313.767	9.125	539 869	145.52	146.62					

[a] Tabulated values for saturated liquid density and vapor pressure were calculated with the equation of state of Bücker and Wagner.[10]

amount (mol) of sample and the calibrated cell volume (L) that was obtained earlier with an uncertainty of 0.012 % from measurements on propane.[8] The densities reported in Table 1 are consistent with the equation of state of Bücker and Wagner.[10] The experimental densities deviate from this equation of state with a standard deviation of 0.0085 %, illustrated in Figure 2 as the dashed lines that represent two standard deviations (± 0.017 %).

Values of the single-phase heat capacity of the liquid are shown in Figure 3 at temperatures from (120 to 345) K with pressures up to 35 MPa. The data were measured along isochores with increasing temperature and pressure. Most of the isochores overlap in their temperature ranges, except at the lowest temperatures (highest densities), where the slope dC_V/dT is observed to increase with increasing density. Figure 4 shows deviations between these measured C_V data relative to calculated values from the equation of state of Bücker and Wagner.[10] Scatter in the C_V data, primarily due to thermally induced noise, increases with temperature but remains within the estimated uncertainty of 0.7 %. The C_V data are (1 to 2) % higher than the equation of state calculations of Bücker and Wagner[10] over the temperature region from (120 to 300) K, decreasing for temperatures above 300 K. Because Bücker and Wagner[10] developed their model by using isobaric heat capacity data in a limited range of pressures up to 0.7 MPa and no isochoric heat capacity data, the observed (1 to 2) % deviations are entirely reasonable. All observed deviations are within the ± (2 to 5) % range of tolerances given by Bücker and Wagner[10] in their Figure 40, which apply to calculations of both isobaric and isochoric heat capacities.

Heat Capacity of the Saturated Liquid. The values measured for the saturated liquid heat capacity, C_σ, of isobutane are given in Table 2 at 94 two-phase states. The average of the initial and final temperatures for each heating interval is given for the temperature (ITS-90) of each data point. Directly measured vapor pressures are not reported in Table 2 because they fall in a low-accuracy range of the pressure transducer. Furthermore, saturated liquid densities were not measured in this work. Therefore, it made the most sense to report thermodynamically consistent vapor pressure and saturated liquid density values in

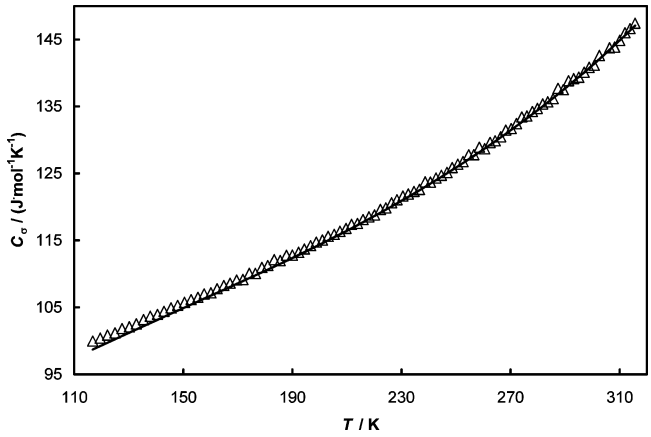

Figure 5. Heat capacities of saturated liquid isobutane (C_σ) from (117 to 316) K: △, present results for $n = 0.70101$ mol; —, calculated with the equation of state of Bücker and Wagner.[10]

Table 2. Those values were calculated with the Bücker and Wagner equation of state,[10] which those authors had shown to reproduce high-accuracy vapor pressure and density data faithfully. Values of the two-phase heat capacity at constant volume ($C_V^{(2)}$) are presented as well as values of the saturated-liquid heat capacity C_σ. We obtained values of C_σ by adjusting the $C_V^{(2)}$ data with the equation given by Rowlinson[18]

$$C_\sigma = C_V^{(2)} - \frac{T}{\rho_\sigma^2}\left(\frac{\mathrm{d}\rho_\sigma}{\mathrm{d}T}\right)\left(\frac{\mathrm{d}P_\sigma}{\mathrm{d}T}\right) + T\left(\frac{1}{\rho_\sigma} - \frac{1}{\rho}\right)\frac{\mathrm{d}^2P_\sigma}{\mathrm{d}T^2} \quad (5)$$

where P_σ and ρ_σ are the pressure and density of the saturated liquid and ρ is the bulk density of the sample residing in the cell. The derivative quantities were all calculated with the equation of state of Bücker and Wagner.[10]

The saturated-liquid heat capacity, C_σ, depends only on the temperature. Figure 5 shows the present data for C_σ at temperatures from (116 to 316) K along with values calculated with the equation of state of Bücker and Wagner.[10] Figure 6 shows relative deviations between the data for C_σ at temperatures from (116 to 316) K and the values calculated with the equation of state of Bücker and Wagner.[10] Low-temperature C_P (less than 0.1 MPa) data that are nearly equal to C_σ are also compared with the present measurements in Figure 6. The C_P data of Aston et al.[12] agree with the present C_σ data to within 1 %, whereas the C_P data of Parks et al.[13] are 0.5 % to 1 % lower than the present C_σ data. Values calculated with the equation of state of Bücker and Wagner[10] agree with the experimental data to within 1 % from the triple-point temperature to 316 K.

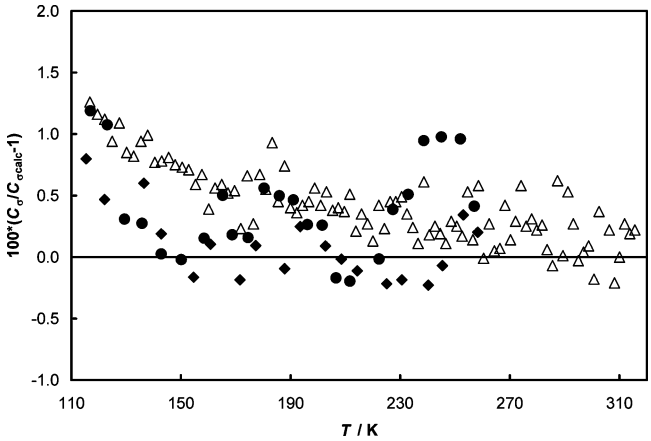

Figure 6. Relative deviations between data for heat capacities of saturated liquid isobutane (C_σ) and values calculated with the equation of state of Bücker and Wagner[10] at temperatures from (117 to 316) K: △, present results for $n = 0.70101$ mol. Deviations for low-temperature C_P (< 0.1 MPa) values that are nearly equal to C_σ are also shown: ●, Aston et al.;[12] ◆, Parks et al.[13]

Derived Vapor Pressure. Accurate measurement of the vapor pressure of a liquid becomes increasingly difficult at temperatures well below the normal boiling point. Glos et al.[17] report the normal boiling point temperature of isobutane to be 261.394 K. Very dilute but volatile impurities in a sample can introduce errors in direct measurements of vapor pressure that are difficult to quantify when the partial pressure of an impurity becomes significant relative to the vapor pressure of the sample. Dynamic techniques such as ebulliometry, effusion, and gas saturation that purge volatile impurities from the gas phase are effective at reducing such errors. It remains difficult to measure pressure accurately for samples that are at a pressure much less than ambient.

Vapor pressure data have been reported at temperatures below 260 K by three groups. The recent work of Glos et al.[17] covered the temperature range from (120 to 340) K with very accurate direct measurement of the vapor pressure. Tickner and Lossing[19] covered the temperature range from (122 to 187) K with vapor pressures determined from isobutane flow through a calibrated orifice quantified by the ion peak intensity from a mass spectrometer. Finally, Aston et al.[12] covered the temperature range from (188 to 262) K by direct measurement of the vapor pressure.

Duarte-Garza and Magee[20] have shown that vapor pressure values can be derived from measurements of the two-phase heat capacity $C_V^{(2)}$ that are described above. This works because $C_V^{(2)}$ values have an excellent internal consistency and have their lowest uncertainty below the normal boiling point because the necessary adjustments to the $C_V^{(2)}$ measurements for vaporization and PV work are less than 0.1 % of the resulting $C_V^{(2)}$ value. Similarly, vapor pressure values derived from these $C_V^{(2)}$ data have a low uncertainty from the triple point of 113.73 K up to the vicinity of the reported normal boiling point of 261.394 K.

In the present work, only a brief summary is given for the technique used to derive vapor pressures from isochoric internal-energy measurements in the two-phase region. A detailed discussion is presented in the original work.[20] The method is based on the expression relating the two-phase internal energy $U^{(2)}(T,V)$ to the vapor pressure

$$\left(\frac{\partial U^{(2)}}{\partial V^{(2)}}\right)_T = T\left(\frac{\mathrm{d}P_\sigma}{\mathrm{d}T}\right) - P_\sigma = T^2\left(\frac{\mathrm{d}(P_\sigma/T)}{\mathrm{d}T}\right) \quad (6)$$

where the subscript σ signifies a quantity evaluated along the liquid−vapor saturation boundary. Because of the linear dependence of $U^{(2)}$ on the molar volume V, the derivative on the left side of eq 6 can be replaced exactly with a finite difference expression

$$\left(\frac{\partial U^{(2)}}{\partial V^{(2)}}\right)_T = \left(\frac{U_2^{(2)} - U_1^{(2)}}{V_2^{(2)} - V_1^{(2)}}\right)_T \quad (7)$$

where subscripts 1 and 2 indicate any two state points within the two-phase region, including the liquid or vapor phase at saturation, and the superscript (2) indicates the bulk property.

In this work, a bulk property is any extensive thermodynamic property of the vapor in equilibrium with the liquid combined in proportion to their phase ratios on a molar basis.

After computing $(\partial U^{(2)}/\partial V^{(2)})_T$ at different temperatures between the triple point and the normal boiling point with eq 7, we can fit eq 6 to these data using a nonlinear regression analysis of the parameters in an equation for $P_\sigma(T)$. As indicated by eq 6, the regression analysis must fit the adjustable parameters in the difference expression $T(\mathrm{d}P_\sigma/\mathrm{d}T) - P_\sigma$. Once an expression for $P_\sigma(T)$ is selected that can accurately represent the vapor pressure over a wide range of temperature, its analytic derivative $(\mathrm{d}P_\sigma/\mathrm{d}T)$ is determined so that the difference expression $T(\mathrm{d}P_\sigma/\mathrm{d}T) - P_\sigma$ depends only on T and the parameters in the equation for $P_\sigma(T)$. In principle, we could have used nonlinear regression to fit a vapor pressure equation to both P_σ and $U^{(2)}$ data simultaneously, but we chose the simpler approach to fit only the $U^{(2)}(T,V)$ data for four reasons, namely: $U^{(2)}$ data vary slowly with temperature, they are only weakly affected by volatile impurities, they extend to temperatures close to the triple point, and we avoid the often difficult problem of assigning optimal fitting weights for the different thermodynamic data. The problem of weights would have been aggravated by the fact that P_σ data typically pass through orders of magnitude in the temperature range of interest.

Experimental values for $U^{(2)}$ at precisely known densities are required to carry out the calculations with eq 7. We use experimental energy-increment data from isochoric (constant $V^{(2)}$) measurements that were performed in this work. Values for $U^{(2)}$ at two or more densities are needed to calculate the change of the bulk internal energy with respect to the bulk molar volume at constant temperature. Because the calorimetric measurements provide the change of internal energy from one density to another, we need additional information at a reference temperature to determine the change of internal energy between two densities. This reference temperature is selected near the normal boiling point, where accurate, direct measurements of the vapor pressure are available.

The value of $(\partial U^{(2)}/\partial V^{(2)})_T$ at the reference temperature can be calculated with eq 6 and vapor pressure data around the reference temperature. Then, the change of internal energy from density 1 to density 2 at that reference temperature can be determined from

$$U_2^{(2)} - U_1^{(2)} = (V_2^{(2)} - V_1^{(2)})\left(\frac{\partial U^{(2)}}{\partial V^{(2)}}\right)_T \tag{8}$$

In the present analysis, we set the internal energy of one of these states $U_1^{(2)}$ to an arbitrary value of zero at the reference temperature. Then, internal energy increments are calculated at each temperature and density on the basis of differences in U from this reference state. Because the present two-phase measurements are at relatively high densities, it is appropriate to select the vapor phase at saturation for the low density state 1 in eq 8. At each temperature considered, $U_1^{(2)}$ and $V_1^{(2)}$ are calculated with the equation of state of Bücker and Wagner[10] at the saturated vapor state with the constraint that $U_1^{(2)} = 0$ at the reference temperature.

A temperature of 245 K was selected as the reference temperature in the present analysis, where vapor pressures can be directly measured with low uncertainty and the properties of the vapor phase approach those of the ideal gas. The accurate vapor pressure data of Glos et al.[17] in the vicinity of 245 K form the basis for analysis of the derived vapor pressure data from the present calorimetric measurements. Bücker and Wagner[10] discuss an equation of the form

$$\ln\left(\frac{P_\sigma}{P_c}\right) = \frac{1}{1-\tau}(C_1\tau + C_2\tau^{1.5} + C_3\tau^{2.5} + C_4\tau^{4.5}) \tag{9}$$

where $\tau = (1 - T/T_c)$, $T_c = 407.81$ K, $P_c = 3629$ kPa, and the C_i are empirical coefficients. Equation 9 accurately represents the best available vapor pressure data for isobutane, including the data of Glos et al.,[17] over a wide range of temperatures from near the triple point to the critical point. Equation 9 is selected as the functional form to represent vapor pressure during the present analysis at temperatures from the triple point to 262 K. The derivative of vapor pressure with respect to temperature, as represented by eq 9, is also required for evaluation of eq 6

$$\frac{\mathrm{d}P_\sigma}{\mathrm{d}T} = -\frac{P_\sigma}{T}\left[\ln\left(\frac{P_\sigma}{P_c}\right) + C_1 + 1.5C_2\tau^{0.5} + 2.5C_3\tau^{1.5} + 4.5C_4\tau^{3.5}\right] \tag{10}$$

Equation 7 was evaluated from two-phase calorimetric data along an isochore at temperatures from (114 to 250) K with the calorimeter filled with $n = 0.70101$ mol isobutane. The change in internal energy along this isochore was determined from a function of temperature fitted to this calorimetric data over the temperature range from (114 to 316) K. The energy needed to increase the temperature of the sample by 1 K is given by

$$\frac{Q}{n\Delta T} = a_0 + a_1T + a_2T^2 + a_3T^3 \tag{11}$$

where Q/J is the energy pulse, n/mol is the amount of substance, and T/K is the sample temperature. The coefficients are given by $a_0 = 8.1730643 \cdot 10^1$, $a_1 = 1.68991666 \cdot 10^{-1}$, $a_2 = -2.29275433 \cdot 10^{-4}$, and $a_3 = 1.07685751 \cdot 10^{-6}$. The change of internal energy along this isochore is given by the expression

$$\Delta U = \int_{T_1}^{T_2} \frac{Q}{n\Delta T}\,\mathrm{d}T \tag{12}$$

Although the exact cell volume varies with temperature and pressure, we may approximate the density as a function of temperature only. The density of this pseudoisochore at temperatures from (116 to 316) K was fit to the equation

$$\rho = b_0 + b_1T + b_2T^2 \tag{13}$$

where ρ is in mol·L^{-1} and the coefficients are given by $b_0 = 5.29491605 \cdot 10^2$, $b_1 = -1.50381468 \cdot 10^{-2}$, and $b_2 = -2.01968831 \cdot 10^{-5}$.

The internal energy of the saturated vapor was calculated from the equation of state of Bücker and Wagner[10] for isobutane. Previous analysis[20] has shown that the results are insensitive to the choice of a gas-phase equation of state as long as it reproduces the correct behavior of the second virial coefficient. A value of $(\partial U^{(2)}/\partial V^{(2)})_T$ was calculated at the reference temperature of 245 K with the ancillary equation for vapor

Table 3. Vapor Pressures, P_σ, Derived from the Present Saturated Liquid Heat Capacity, C_σ, Data for Isobutane at Temperatures from (113.73 to 261) K[a]

T	P	$P_{\mathrm{calcd},\sigma}$	ΔP_σ	$100\Delta P_\sigma/P_\sigma$	T	P	$P_{\mathrm{calcd},\sigma}$	ΔP_σ	$100\Delta P_\sigma/P_\sigma$
K	Pa	Pa	Pa	%	K	Pa	Pa	Pa	%
113.730	0.02279	0.02192	0.00087	3.969	189.000	1626.41049	1623.32844	3.08205	0.190
115.000	0.03158	0.03043	0.00116	3.800	191.000	1915.53605	1912.25654	3.27951	0.171
117.000	0.05198	0.05020	0.00178	3.547	193.000	2247.24439	2243.77333	3.47106	0.155
119.000	0.08400	0.08131	0.00269	3.310	195.000	2626.43606	2622.78122	3.65484	0.139
121.000	0.13340	0.12941	0.00400	3.088	197.000	3058.40015	3054.57098	3.82916	0.125
123.000	0.20838	0.20255	0.00583	2.879	199.000	3548.82741	3544.83487	3.99254	0.113
125.000	0.32041	0.31204	0.00838	2.684	201.000	4103.82266	4099.67888	4.14378	0.101
127.000	0.48536	0.47351	0.01184	2.501	203.000	4729.91612	4725.63412	4.28201	0.091
129.000	0.72481	0.70831	0.01650	2.329	205.000	5434.07386	5429.66713	4.40673	0.081
131.000	1.06781	1.04514	0.02266	2.169	207.000	6223.70714	6219.18925	4.51788	0.073
133.000	1.55288	1.52217	0.03071	2.018	209.000	7106.68070	7102.06485	4.61585	0.065
135.000	2.23060	2.18952	0.04108	1.876	211.000	8091.32001	8086.61853	4.70148	0.058
137.000	3.16655	3.11227	0.05428	1.744	213.000	9186.41729	9181.64115	4.77614	0.052
139.000	4.44488	4.37402	0.07086	1.620	215.000	10 401.23649	10 396.39485	4.84164	0.047
141.000	6.17249	6.08104	0.09144	1.504	217.000	11 745.51713	11 740.61685	4.90027	0.042
143.000	8.48380	8.36709	0.11672	1.395	219.000	13 229.47696	13 224.52222	4.95474	0.037
145.000	11.54633	11.39893	0.14740	1.293	221.000	14 863.81362	14 858.80551	5.00812	0.034
147.000	15.56691	15.38264	0.18426	1.198	223.000	16 659.70510	16 654.64135	5.06374	0.030
149.000	20.79878	20.57071	0.22807	1.109	225.000	18 628.80922	18 623.68406	5.12516	0.028
151.000	27.54952	27.26989	0.27963	1.025	227.000	20 783.26210	20 778.06614	5.19597	0.025
153.000	36.18970	35.85000	0.33970	0.948	229.000	23 135.67561	23 130.39592	5.27969	0.023
155.000	47.16255	46.75353	0.40902	0.875	231.000	25 699.13386	25 693.75426	5.37960	0.021
157.000	60.99438	60.50612	0.48826	0.807	233.000	28 487.18896	28 481.69039	5.49857	0.019
159.000	78.30589	77.72787	0.57802	0.744	235.000	31 513.85573	31 508.21692	5.63881	0.018
161.000	99.82434	99.14557	0.67877	0.685	237.000	34 793.60588	34 787.80420	5.80168	0.017
163.000	126.39642	125.60558	0.79084	0.630	239.000	38 341.36125	38 335.37381	5.98743	0.016
165.000	159.00203	158.08761	0.91443	0.578	241.000	42 172.48660	42 166.29166	6.19494	0.015
167.000	198.76863	197.71912	1.04952	0.531	243.000	46 302.78172	46 296.36030	6.42142	0.014
169.000	246.98628	245.79037	1.19591	0.487	245.000	50 748.47300	50 741.81088	6.66212	0.013
171.000	305.12326	303.77007	1.35319	0.445	247.000	55 526.20462	55 519.29458	6.91004	0.012
173.000	374.84214	373.32143	1.52071	0.407	249.000	60 653.02933	60 645.87377	7.15557	0.012
175.000	458.01628	456.31867	1.69760	0.372	251.000	66 146.39886	66 139.01269	7.38617	0.011
177.000	556.74657	554.86379	1.88278	0.339	253.000	72 024.15413	72 016.56807	7.58606	0.011
179.000	673.37842	671.30350	2.07492	0.309	255.000	78 304.51524	78 296.77940	7.73584	0.010
181.000	810.51883	808.24631	2.27252	0.281	257.000	85 006.07136	84 998.25919	7.81217	0.009
183.000	971.05340	968.57949	2.47391	0.255	259.000	92 147.77047	92 139.98306	7.78742	0.008
185.000	1158.16323	1155.48597	2.67726	0.232	261.000	99 748.90918	99 741.27984	7.62933	0.008
187.000	1375.34164	1372.46101	2.88063	0.210					

[a] These derived values are compared with the values $P_{\mathrm{calcd},\sigma}$ calculated with the vapor pressure expression of Bücker and Wagner.[10]

pressure of Bücker and Wagner[10] for isobutane. Application of the method described above to calculate vapor pressures from the measured internal energy increments resulted in optimum coefficients for the vapor pressure expression of eq 9. These coefficients are given by $C_1 = -6.90872652$, $C_2 = 1.52675920$, $C_3 = -1.53031020$, and $C_4 = -2.36936121$. It must be emphasized that these coefficients are optimized for the temperature range from the triple point to 262 K, and eq 9 should not be used with these coefficients at temperatures above 262 K. At temperatures above 262 K, the ancillary expression of Bücker and Wagner[10] is more accurate. Table 3 provides the vapor pressures calculated from internal energy increments, along with values calculated with the ancillary equation of Bücker and Wagner[10] for isobutane. Figure 7 shows deviations between the present vapor pressures derived from C_σ, along with data from the literature, relative to the ancillary equation of Bücker and Wagner[10] at temperatures from the triple point to 262 K. We note that the present values are in excellent agreement with the direct measurements of Glos et al.[17] at temperatures up to 262 K. Because the ancillary equation of Bücker and Wagner[10] is based on their own vapor pressure measurements,[17] a high level of agreement with our derived vapor pressures provides strong evidence that any inconsistencies between them are inconsequential. This finding is most important for the calculations of C_σ by using eq 5 because two important derivatives in this equation were calculated with the ancillary equation of Bücker and Wagner.[10] Figure 8 focuses

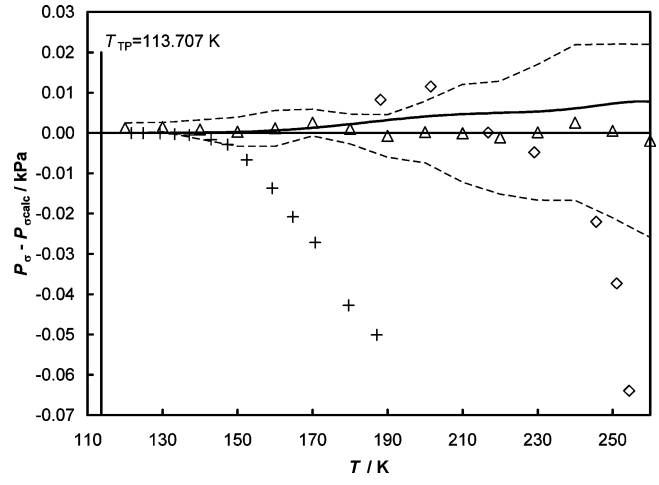

Figure 7. Deviations between vapor pressures (P_σ) and the vapor pressure expression of Bücker and Wagner[10] for isobutane ($P_{\sigma,\mathrm{calcd}}$) at temperatures from (113.707 to 260) K: —, P_σ values derived from the present saturated liquid heat capacity, C_σ, data. Published data for P_σ are also shown: △, Glos et al.;[17] +, Tickner and Lossing;[19] ◇, Aston et al.;[12] ---, uncertainty bounds for the data of Glos et al.[17]

on the vapor pressure deviations at the lowest temperatures, from the triple point to 160 K. The present values are in slightly better agreement with the data of Tickner and Lossing[19] (orifice-mass selective detector) than the direct pressure measurements of Glos

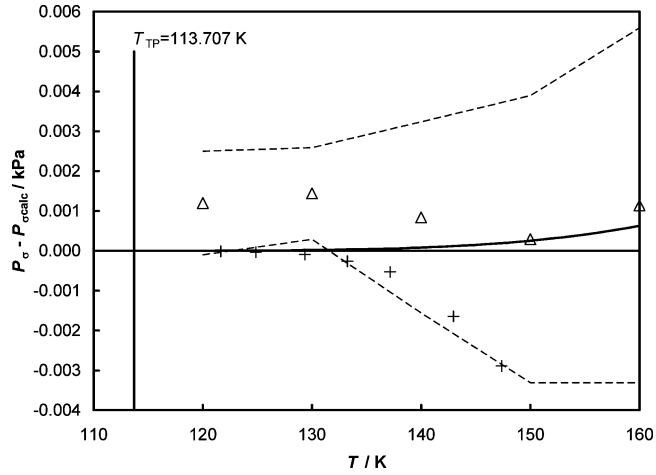

Figure 8. Deviations between vapor pressures (P_σ) and the vapor pressure expression of Bücker and Wagner[10] for isobutane ($P_{\sigma,\mathrm{calcd}}$) at temperatures from (113.707 to 160) K: —, P_σ values derived from the present saturated liquid heat capacity, C_σ, data. Published data for P_σ are also shown: △, Glos et al.;[17] +, Tickner and Lossing;[19] ---, uncertainty bounds for the data of Glos et al.[17]

et al.[17] at temperatures below 136 K. It appears that this indirect technique was less sensitive to impurities at the lowest pressures. However, agreement is excellent (< 0.2 Pa) and within claimed uncertainties for all measurements at temperatures below 140 K. It is also apparent in Figure 8 that there were no data available at temperatures below 120 K prior to the present work. On the basis of the present vapor pressure results, the triple-point pressure of isobutane is 0.023 Pa at the triple-point temperature of 113.73 K, reported above. This agrees well with the value of 0.02 Pa reported by Glos et al.[17]

Assessment of Uncertainties. Uncertainty in C_V is limited by the uncertainty of the temperature increase measurement and the change-of-volume work adjustment. In the following discussion, the definition for the expanded uncertainty, which is two times the standard uncertainty, corresponds to a coverage factor $k = 2$ and thus a two standard deviation estimate. Recent triple-point measurements of argon[8] (Supporting Information) indicate that the calibration of the platinum resistance thermometer presently has an uncertainty of 0.003 K near the ITS-90 fixed point for the triple point of argon (83.8058 K). Different sources of uncertainty, including calibration of the platinum resistance thermometer, radiation to or from the thermometer head, and shifts in the resistance at temperature scale fixed points contribute to an expanded uncertainty of 0.01 at 100 K to 0.03 at 345 K for the absolute temperature measurement during C_V measurements. The uncertainty of the temperature increase also depends on reproducibility of temperature measurements. Between heating intervals, temperatures are measured while the cell temperature drifts linearly with time for a period of 20 min. The temperatures assigned to the beginning (T_1) and to the end (T_2) of a heating interval are determined by extrapolation of a linear temperature drift (approximately $((-1 \cdot 10^{-3})$ to $(0.5 \cdot 10^{-3}))$ K·min^{-1}) to the midpoint time of the interval. This procedure leads to an uncertainty of (0.01 to 0.04) K for the extrapolated temperatures T_1 and T_2, depending on the standard deviation of the linear fit. In all cases, values from (0.002 to 0.006) K were obtained for the uncertainty of the temperature rise, $\Delta T = T_2 - T_1$. For a typical experimental value of $\Delta T =$ 4 K, this corresponds to a relative uncertainty of between 0.05 % and 0.15 %.

The uncertainty of the change-of-volume work adjustment has a larger influence on the single-phase values because two-phase experiments are performed over a smaller pressure interval. The ratio of change-of-volume work to total applied heat ranges from 0.11 for the highest density isochore to 0.005 at the lowest densities. Estimated uncertainties of 2.3 % to 3.0 % in the change-of-volume work adjustment are due to both the deviation of the calculated pressure derivatives and the uncertainty of the volume change. This leads to a relative uncertainty of 0.2 % in C_V for the lowest density isochore up to 0.3 % for the highest density.

The energy applied to the calorimeter is the integral of the product of voltage and current from the initial to the final heating time. Voltage and current are measured 20 times during a heating interval, which lasts 20 min. The measurements of the electrical quantities have a relative uncertainty of 0.01 %. However, we must account for the effect of radiation heat losses or gains, which occur when a time-dependent lag of the controller leads to a small temperature difference of about 20 mK between the cell and the radiation shield at the beginning and end of a heating period. Because heat transfer by radiation is proportional to $(T_1^4 - T_2^4) \approx 4 \cdot T^3 \cdot \Delta T$, radiation losses should increase substantially with the cell temperature. Therefore, the relative uncertainty in the applied heat is estimated to be 0.02 % for lower temperatures and up to 0.10 % for the highest temperatures. This leads to a relative uncertainty in C_V between 0.04 % and 0.2 %.

The energy applied to the empty calorimeter has been measured in repeated experiments and fitted to a function of temperature;[3] its relative uncertainty is less than 0.02 %. Its influence on the uncertainty of the heat capacity is reduced because the ratio of the heat applied to the empty calorimeter to the total heat varies only from 0.35 to 0.70 for the single-phase runs and from 0.61 to 0.62 for the two-phase runs. The mass of each sample was determined with a relative uncertainty of 0.01 % by differential weighing before and after trapping the sample in the collection cylinder. The density calculated from this mass and the cell volume has a relative uncertainty of 0.03 %. For pressures, the uncertainty of 7 kPa for the pressure transducer is added to the cross term for the pressure derivative in the change-of-volume work adjustment. However, the uncertainty of neither P nor ρ contributes appreciably to the combined uncertainty for molar heat capacity. When the various sources of experimental uncertainty are combined using a root-sum-of-squares formula, the expanded uncertainty (i.e., a coverage factor $k = 2$ and thus a two-standard deviation estimate) is estimated to be 0.7 % for C_V, 0.5 % for $C_V^{(2)}$, and 0.7 % for C_σ.

Conclusions

Calorimetric measurements were conducted on liquid isobutane in equilibrium with its vapor and on compressed liquid isobutane along isochores. The heat capacity, C_V, was measured as a function of temperature and density at 171 single-phase and 94 two-phase states for isobutane. Molar heat capacity results are reported for two-phase ($C_V^{(2)}$), saturated liquid (C_σ), and single-phase (C_V) isochores. Temperatures ranged from the triple point of isobutane, near 114 K, to the upper temperature limit of the calorimeter of 345 K at pressures up to 35 MPa. Vapor pressure data are reported that are based on measurements of $C_V^{(2)}$ along a two-phase isochore. Measurements were also made to determine the triple-point temperature of (113.707 ± 0.030) K and enthalpy of fusion of (4494 ± 20) J·mol^{-1} for isobutane near its triple point. The principal sources of uncertainty are the temperature rise measurement and the change-of-volume work adjustment. The expanded uncertainty

(i.e., a coverage factor $k = 2$ and thus a two-standard deviation estimate) for values of $C_V^{(2)}$ is estimated to be 0.5 %, for C_σ it is 0.7 %, and for C_V it is 0.7 %. These measurements agree well with published heat capacity measurements and with the Helmholtz free energy model of Bücker and Wagner,[10] who had developed their model independently of this study. The present study suggests that on the basis of the presently available experimental thermodynamic data, a revision of the model of Bücker and Wagner[10] is not needed at this time.

Acknowledgment

We thank Eric Lemmon and Mark McLinden for generous technical assistance and helpful discussions. We thank JCED Editors for organizing the "William A. Wakeham Festschrift" to which we are honored to contribute this manuscript. Above all, we express our appreciation to Bill Wakeham for many collegial discussions, numerous scientific collaborations, and most of all, for a steadfast friendship now spanning many years. We extend our warmest wishes to Bill on the occasion of his retirement from University of Southhampton and wish him all the best as he enters into new scientific endeavors.

Supporting Information Available:

Measurement of the triple-point temperature of pure (0.999999 mol fraction) argon and its offset of 3 mK above that of the fixed point on the ITS-90 temperature scale. This material is available free of charge via the Internet at http://pubs.acs.org.

Literature Cited

(1) Goodwin, R. D. Apparatus for determination of pressure−density−temperature relations and specific heats of hydrogen to 350 atm at temperatures above 14 degrees K. *J. Res. Natl. Bur. Stand.* **1961**, *65C*, 231–243.
(2) Younglove, B. A. The specific heats, C_σ and C_V, of compressed and liquefied methane. *J. Res. Natl. Bur. Stand.* **1974**, *78A*, 401–410.
(3) Roder, H. M. Measurements of the specific heats, C_σ and C_V, of dense gaseous and liquid ethane. *J. Res. Natl. Bur. Stand.* **1976**, *80A*, 739–759.
(4) Mayrath, J. E.; Magee, J. W. Measurements of molar heat capacity at constant volume: $C_{V,m}\{x\mathrm{CH_4} + (1-x)\mathrm{C_2H_6}$, $T = 100$ to 320 K, $p <$ 35 MPa$\}$. *J. Chem. Thermodyn.* **1989**, *21*, 499–513.
(5) Goodwin, R. D. Specific heats of saturated and compressed liquid propane. *J. Res. Natl. Bur. Stand. (U.S.)* **1978**, *83*, 449–458.
(6) Magee, J. W. Molar heat capacity (C_V) for saturated and compressed liquid and vapor nitrogen from 65 to 300 K at pressures to 30 MPa. *J. Res. Natl. Inst. Stand. Technol.* **1991**, *96*, 725–740.
(7) Magee, J. W.; Lüddecke, T. O. D. Molar heat capacity at constant volume of *n*-butane at temperatures from 140 to 342 K and at pressures to 33 MPa. *Int. J. Thermophys.* **1998**, *19*, 129–144.
(8) Perkins, R. A.; Sanchez-Ochoa, J. C.; Magee, J. W. Thermodynamic properties of propane. II. Molar heat capacity at constant volume from 85 to 345 K with pressures to 30 MPa. *J. Chem. Eng. Data* **2009**, accepted.
(9) Goodwin, R. D.; Weber, L. A. Specific heats of oxygen at coexistence. *J. Res. Natl. Bur. Stand.* **1969**, *73A*, 1–13.
(10) Bücker, D.; Wagner, W. Reference equations of state for the thermodynamic properties of fluid phase *n*-butane and isobutane. *J. Phys. Chem. Ref. Data* **2006**, *35* (2), 929–1019.
(11) Wieser, M. E. Atomic weights of the elements 2005 (IUPAC technical report). *Pure Appl. Chem.* **2006**, *78*, 2051–2066.
(12) Aston, J. G.; Kennedy, R. M.; Schumann, S. C. The heat capacity and entropy, heats of fusion and vaporization and the vapor pressure of isobutane. *J. Am. Chem. Soc.* **1940**, *62*, 2059–2063.
(13) Parks, G. S.; Shomate, C. H.; Kennedy, W. D.; Crawford, B. L. The entropies of *n*-butane and isobutane with some heat capacity data for isobutane. *J. Chem. Phys.* **1937**, *5*, 359–363.
(14) Das, T. R.; Reed, C. O., Jr.; Eubank, P T. PVT surface and thermodynamic properties of isobutane. *J. Chem. Eng. Data* **1973**, *18*, 253–262.
(15) Rossini, F. D.; Pitzer, K. S.; Arnett, R. L.; Braun, R. M.; Pimentel, G. C. *Selected Values of Physical and Thermodynamic Properties of Hydrocarbons and Related Compounds*; Carnegie Press: Pittsburgh, PA, 1953.
(16) Francis, A. W. Relations between physical properties of paraffin hydrocarbons. *Ind. Eng. Chem.* **1941**, *33*, 554–560.
(17) Glos, S.; Kleinrahm, R.; Wagner, W. Measurement of the (p,ρ,T) relation of propane, propylene, *n*-butane, and isobutane in the temperature range from (95 to 340) K at pressures up to 12 MPa using an accurate two-sinker densimeter. *J. Chem. Thermodyn.* **2004**, *36*, 1037–1059.
(18) Rowlinson, J. S. *Liquids and Liquid Mixtures*; Butterworths: London, 1969.
(19) Tickner, A. W.; Lossing, F. P. The measurement of low vapor pressures by means of a mass spectrometer. *J. Phys. Colloid Chem.* **1951**, *55*, 733–40.
(20) Duarte-Garza, H. A.; Magee, J. W. Subatmospheric vapor pressures evaluated from internal-energy measurements. *Int. J. Thermophys.* **1997**, *18*, 173–193.

Received for review February 4, 2009. Accepted April 23, 2009.

JE9001575